Biophysical Journal Volume 73 November 1997 2404–2415

The Dielectric Properties of Water within Model Transbilayer Pores

M. S. P. Sansom, G. R. Smith, C. Adcock, and P. C. Biggin
Laboratory of Molecular Biophysics, University of Oxford, Oxford OX1 3QU, England

ABSTRACT Ion channels contain extended columns of water molecules within their transbilayer pores. The dynamic properties of such intrapore water have been shown to differ from those of water in its bulk state. In previous molecular dynamics simulations of two classes of model pore (parallel bundles of Ala_{20} α-helices and antiparallel barrels of Ala_{10} β-strands), a substantially reduced translational and rotational mobility of waters was observed within the pore relative to bulk water. Molecular dynamics simulations in the presence of a transpore electrostatic field (i.e., a voltage drop along the pore axis) have been used to estimate the resultant polarization (due to reorientation) of the intrapore water, and hence to determine the local dielectric behavior within the pore. It is shown that the local dielectric constant of water within a pore is reduced for models formed by parallel α-helix bundles, but not by those formed by β-barrels. This result is discussed in the context of electrostatics calculations of ion permeation through channels, and the effect of the local dielectric of water within a helix bundle pore is illustrated with a simple Poisson-Boltzmann calculation.

INTRODUCTION

Membrane-spanning pores are present in ion channels (Unwin, 1989; Hille, 1992), in bacterial porins (Cowan et al., 1992) and toxins (Song et al., 1996), and in a number of related transport proteins (e.g., aquaporins; Engel et al., 1994; Walz et al., 1995). In all of these integral membrane proteins, an irregular central column of water molecules is believed to be surrounded by a pore lining formed from membrane-spanning polypeptide chains (Kreusch and Schulz, 1994; Montal, 1995; Unwin, 1995). In many ion channels the pore is formed by a bundle of approximately parallel α-helices. Examples of such channels include the nicotinic acetylcholine receptor (Unwin, 1993, 1995; Sankararamakrishnan et al., 1996), phospholamban (Adams et al., 1995; Arkin et al., 1995), influenza M2 protein (Sansom and Kerr, 1993), and several channel-forming peptides (Sansom, 1991), such as alamethicin (Sansom, 1993a,b; Breed et al., 1997) and *Staphylococcus aureus* δ-toxin (Mellor et al., 1988; Kerr et al., 1995, 1996).

To understand the molecular basis of transport through a transmembrane pore, it is necessary to understand the physical properties of water within that pore. Simulation studies of a number of channel models (Chiu et al., 1991; Green and Lewis, 1991; Roux and Karplus, 1994; Engels et al., 1995; Sancho et al., 1995; Breed et al., 1996; Mitton and Sansom, 1996; Singh et al., 1996) have suggested that pore water differs in its dynamic properties from bulk water, exhibiting decreased translational and rotational mobility. Furthermore, simulations on water within idealized channels (Lynden-Bell and Rasaiah, 1996; Sansom et al., 1996) suggest that cylindrical solvation shells may be formed inside the channel walls. Such perturbations of the dynamic and structural behavior of intrapore water may influence the local dielectric constant of the solvent and hence the strength of the electrostatic field experienced within a pore. The appropriate value of the solvent dielectric to use within a transbilayer pore is an important parameter in Poisson-Boltzmann (PB) calculations of electrostatic properties of ion channels (Karshikoff et al., 1994; Sankararamakrishnan et al., 1996) and in more general electrostatic treatments of ion permeation through channels (Partenskii and Jordan, 1992a; Syganow and von Kitzing, 1995; Chen et al., 1997). The differences between bulk water and the pore water/channel system can be expected to manifest themselves primarily as nonlinearities and nonlocalities in the dielectric response. We concentrate in this paper almost entirely on the former. We also remark that the question of what dielectric constant is appropriate in a Poisson-Boltzmann calculation depends on what is being calculated; the approximations inherent in a continuum approximation affect different quantities in different ways. We shall concentrate on definitions appropriate to ion permeation, but other calculations, for example, of Born solvation energy, would require a different treatment (Partenskii and Jordan, 1992a).

As there are few experimental measurements of the solvent dielectric within a pore (Gutman et al., 1992), it is appropriate to approach this problem via simulations. A number of studies have shown that molecular dynamics (MD) simulations may be used to investigate the dielectric properties of liquid water (Neumann, 1986; Alper and Levy, 1989; Simonson, 1996). More recently, MD simulations have been used to estimate spatial variations in the dielectric constant of several globular proteins (Smith et al., 1993; Simonson and Perahia, 1995a,b) and to explore the dielectric response of bovine pancreatic trypsin inhibitor to an external electrostatic field (Xu et al., 1996). In the current investigation, similar techniques are used to estimate the local dielectric constant within the pores of two simplified models of ion channels. The results indicate that water

Received for publication 25 April 1997 and in final form 4 August 1997.

Address reprint requests to Dr. Mark S. P. Sansom, Laboratory of Molecular Biophysics, The Rex Richards Building, University of Oxford, South Parks Road, Oxford OX1 3QU, England. Tel.: +44-1865-275371; Fax: +44-1865-275182; E-mail: mark@biop.ox.ac.uk.

0006-3495/97/11/2404/12 $2.00

within a pore formed by a parallel bundle of α-helices exhibits a dielectric constant significantly lower than that of bulk water. We may hope that a single effective dielectric will be appropriate within the pore (for any one type of calculation), for if ϵ has to vary spatially within it, then the simplicity of using continuum-dielectric models will be lost.

THEORY AND METHODS

General

Simulations were performed using Charmm (Brooks et al., 1983), version 23f3, run on DEC2100 workstations. Other calculations were carried out on Silicon Graphics R3000 and R4000 workstations. Structure diagrams were drawn using Molscript (Kraulis, 1991).

MD simulations

In the MD simulations the water model employed was the TIP3P three-site model (Jorgensen et al., 1983) with partial charges $q_O = -0.834$ and $q_H = +0.417$, as in the PARAM19 parameter set of Charmm. The latter parameter set was used for the protein, which was represented by using the extended atom approximation for nonpolar carbons. Model pores were solvated with preequilibrated boxes of TIP3P water molecules. Water molecules were selected so that the central pore and the cap regions at either mouth of the pore were solvated, but such that no water molecules were present on the bilayer-exposed faces of the pores. Details of the MD simulations were as in Breed et al. (1996), with the exception that a voltage gradient (i.e., E-field) was imposed along the pore (z) axis (see below). The simulation protocol was as follows. Solvated model pores were energy minimized before MD simulations, using a four-stage energy minimization: 1) 1000 cycles of adopted basis Newton-Raphson (ABNR) minimization with the protein atoms fixed; 2) 1000 cycles of ABNR with the protein backbone atoms restrained; 3) 1000 cycles of ABNR with weak restraints on the protein Cα atoms only; and 4) 1000 cycles of ABNR with no positional restraints. The external electric field was not imposed during the minimization. During the MD simulations restraints were applied to water molecules to prevent them from evaporating from the ends of the pore. These took the form of a cylindrical "well" (wall height 7.5 kcal/mol) within which the pore water molecules were contained. The radius and length of the cylinder were such that the restraining force was experienced not by waters within the pore, but only by those at the surface of the caps. We note that comparable restraining potentials have been used in simulations of water within channels formed by, e.g., gramicidin (Chiu et al., 1991) and by a Na^+ channel model (Singh et al., 1996).

MD simulations used a 1-fs time step. The system was heated from 0 to 300 K in 6 ps (5 K, 0.1-ps steps) and equilibrated for 9 ps at 300 K by rescaling velocities every 0.1 ps. Total simulation times varied between 100 ps and 500 ps (see Table 1). Coordinate sets were saved every picosecond for later analysis. Nonbonded interactions (both electrostatic and van der Waals) between distant atoms were truncated by using a shift function (Brooks et al., 1983) with a cutoff of 13.0 Å.

A voltage gradient along the z axis was added to the Charmm potential function, essentially as described by Biggin and Sansom (1996). As illustrated in Fig. 1, the voltage was set to $V = 0$ mV for $z < -30$ Å and to $V = \Delta V$ for $z > +30$ Å. Thus the field strength for the region between was $\Delta V/60$ mV/Å. MD simulations in the presence of an external electric field all started from the system minimized in the absence of such a field. A test simulation in which the field was also applied during the minimization did not yield any significant difference in the outcome of the simulation. All of the fields applied were static with respect to time.

Analysis

Water dipole orientations were analyzed from coordinate sets saved during the simulations. The orientation of water molecules relative to the pore (z) axis was measured in terms of the projection onto the z axis of the dipole moment of each water, μ_Z. Note that for an ideal TIP3P water molecule with its dipole exactly parallel to the z axis, $\mu_Z = 2.35$ D.

The dipolar component of the dielectric constant of a medium can be obtained from the polarization in the presence of an applied electrostatic field. Note that in the following discussion we use E (or, where necessary for clarity, E_{TOT}) for the total electric field, E_0 for some particular value of this field, E_{EXT} for the externally applied E-field, and E_p for the field experienced by the water when $E_{EXT} = 0$ (so, in general, $E = E_p + E_{EXT}$). For a system where the dielectric constant comes from rotational reorientation of dipoles, it is possible (neglecting dipole-dipole interactions) to calculate $P(E)$, i.e., the polarization as a function of the total electrostatic field E. The result is

TABLE 1 Systems and simulations

System	No. of waters	E_{EXT} (mV/A)	Duration of simulation (ps)
BN8S8	293	0	500
		+20	500
		−20	500
AN5	160	0	500
		+20	500
		+50	300
		+60	300
		+75	300
		+100	300
		+200	100
R6L60	245	0	100
		+13.3	100
		+20	100
		−20	100

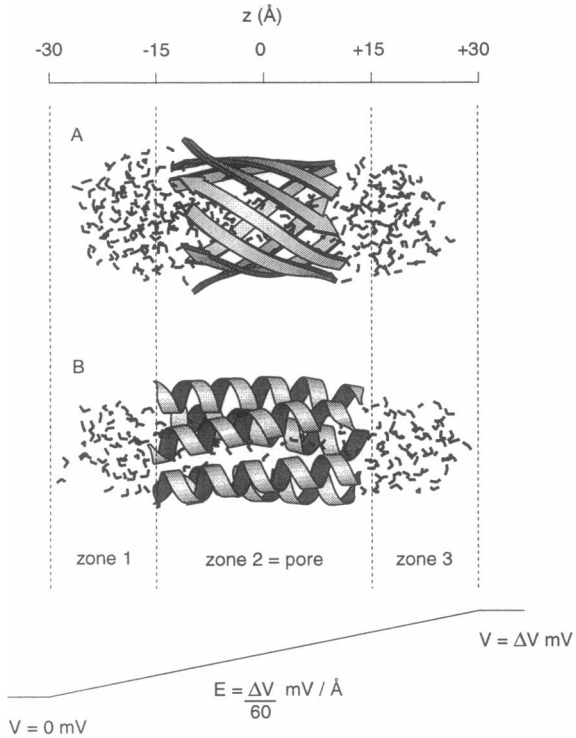

FIGURE 1 Diagram of the systems used in these simulations. The upper structural diagram (drawn using Molscript; Kraulis, 1991) shows model BN8S8, with the β-strands as arrows and the water molecules in "bonds" format. The lower diagram shows model AN5, with the α-helices as ribbons. Zones 1, 2, and 3 are defined, with zone 2 ($|z| < 15$ Å) corresponding to the pore. The line below indicates the voltage gradient (i.e., E_{EXT}) applied across the model pores.

expected to be a Langevin function,

$$P(E) = \left(\frac{\mu_0}{v_w}\right)(\coth(x) - 1/x) \tag{1}$$

where $x = \mu_0 E/k_B T$, μ_0 is the dipole moment of a water molecule, and v_w is its volume. A suitably scaled version of this function is shown in Fig. 2. Examination of this shows how the Langevin function includes the nonlinear aspect of the dielectric response, i.e., the tendency toward dielectric saturation at very high field strength. The use of a Langevin function to describe the polarization of water is the basis of the protein dipole, Langevin dipole, (PDLD) method (Warshel and Åqvist, 1991). Although our use of it will be different, staying within the framework of the Poisson equation, Warshel has already shown (Åqvist and Warshel, 1989) that the results of electrostatics calculations on channels are effected by the treatment of water in this way. Even for systems like water, where interactions between molecules are strong, an equation of this form is expected to apply, although with a different prefactor (Watts, 1981a). If this equation is linearized around $E = 0$, we obtain

$$P(E) = E\left.\frac{dP}{dE}\right|_0 \tag{2}$$

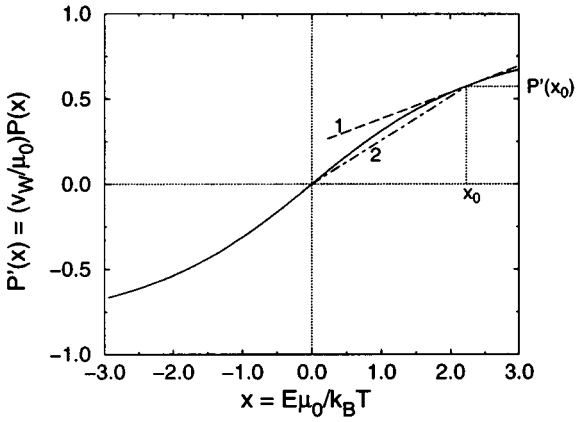

FIGURE 2 Langevin function (see Eq. 1) representing the polarization, P, as a function of the total electrostatic field, x, both suitably scaled. The two broken lines represent (*1*) the gradient $dP/dx|_{x0}$, corresponding to ϵ' in Eq. 5; and (*2*) the gradient $P'(x_0)/x_0$, corresponding to ϵ in Eq. 7.

which is consistent with the familiar

$$P(E) = \epsilon_0(\epsilon - 1)E \tag{3}$$

with the identification $dP/dE|_0 \equiv \epsilon_0(\epsilon - 1)$. This approximation is likely to be the appropriate one for analysis of the β-barrel models, where the protein produces no strong net field and we shall be looking at the response to external fields that are much less than $k_B T/\mu_0$. Indeed, it is valid to a good accuracy up to field strengths such that $\langle \mu_Z \rangle \approx \mu_0/2$. It should be noticed that direct differentiation of Eq. 1 leads to a prediction for ϵ in terms of atomic parameters.

However, it is also possible to linearize Eq. 1 around some higher field strength E_0, by using Taylor's theorem:

$$P(E) \approx P(E_0) + (E - E_0)\left.\frac{dP}{dE}\right|_{E_0} \tag{4}$$

where, by analogy with Eq. 1, we may identify $dP/dE|_{E0}$ with $\epsilon_0(\epsilon'_{LOCAL}(E_0) - 1)$, thus defining the local field-dependent effective dielectric constant $\epsilon'_{LOCAL}(E)$. This gives

$$P(E) = P(E_0) + \epsilon_0(\epsilon'_{LOCAL} - 1)(E - E_0) \tag{5}$$

This form of the equation will be appropriate in the analysis of helix-bundle models, where the total field in the pore E has a large fixed contribution E_p from the protein so, in the case of zero external field, $E_0 = E_p$.

How may one apply this approach to the analysis of simulations? By measurement of the orientations of water dipoles, one may estimate $P = \Sigma\mu/\text{volume}$ i.e., the (orientational) polarization, in response to the external electric field, $E_{EXT} = \Delta V/d$. In the current study this E-field is applied along z, and the polarization is also measured along this axis, giving

$$P_z = \frac{\langle \mu_z \rangle}{v_w} \tag{6}$$

where $\langle \mu_Z \rangle$ is the average z-projection of the dipole moment of a water molecule within a given region of space, and where $v_W = 29.9$ Å^3 is the volume occupied by a water molecule. The total electric field E is in general not known, because E_p may not be zero. However, by varying E_{EXT} and measuring P_Z, a curve with the form of Fig. 2 will be obtained, crossing the horizonal axis where $E_{EXT} = -E_p$. At any particular point $(E_0, P_Z(E_0))$ on the curve of P versus E, there are two natural "gradients" to consider, $dP/dE|_{E0}$ and $P_Z(E_0)/E_0$, as shown in Fig. 2. The first of these was identified with ϵ'_{LOCAL} above, and the second can also be used in the same way to define a (different) effective dielectric ϵ_{LOCAL}; explicitly, we obtain

$$\epsilon_{LOCAL} = 1 + \frac{1}{\epsilon_0} \cdot \frac{P_Z(E_0)}{E_0} \tag{7}$$

Thus in either case measurement of P_Z as a function of E leads to an estimate of ϵ_{LOCAL}. We defer detailed discussion of the significance and use of ϵ'_{LOCAL} and ϵ_{LOCAL} to the end of the Results section.

Poisson-Boltzmann electrostatics

An approximate electrostatic potential within an α-helix bundle was calculated via numerical solution of the Poisson-Boltzmann equation, using the program UHBD (Davis et al., 1991). The protein dielectric was set to $\epsilon = 2$, and the water dielectric in the "bulk" phase (i.e., outside the pore) was set to $\epsilon = 78$. The dielectric within the pore (i.e., within the pore lumen between $z = -15$ and $+15$ Å) was set to ϵ_{LOCAL}. The α-helix bundle was embedded in a low-dielectric ($\epsilon = 2$) slab to mimic the effect of the surrounding protein and lipid bilayer. The ionic strength was set to zero, and a $(65)^3 \times 1$ Å grid was used. The partial atomic charges and radii used in these calculations were the same as in the MD simulations (i.e., the standard Charmm values). Electrostatic energy profiles were obtained by calculating the energy of a $+1e$ probe charge placed at successive positions along the central (z) axis of the pore.

RESULTS

Systems and simulations

To probe the dielectric behavior of water in two classes of pore environment, two simplified model channels, which have formed the basis of earlier simulations of water within channels (Breed et al., 1996), were explored: 1) an eight-stranded antiparallel β-barrel (shear number $S = 8$) of Ala_{10} β-strands, referred to hereafter as model BN8S8; and 2) a parallel bundle of five Ala_{20} α-helices, model AN5. Both of these models were solvated within and at the mouths of their respective pores. To allow comparison with a similar number of waters without any protein, a cylindrical cavity (with repulsive, i.e., hydrophobic, walls; Sansom et al., 1996) of length 60 Å and radius 6 Å was employed (model R6L60).

These three systems were used in simulations without and with a external transpore E-field. The way in which the field was applied is illustrated in Fig. 1. In each case the long axis of the pore was placed parallel to the z axis, with the center of the system at $z = 0$. Thus in each case the pores extended approximately over $|z| < 15$ Å. As described before, an external electric field of $E_{EXT} = \Delta V/60$ mV/Å was applied along the z axis.

The MD simulations run using these systems are summarized in Table 1. For all three systems, simulations in the absence of an applied electric field and simulations with a relatively low field strength ($E_{EXT} = 20$ mV/Å) were run. For the α-helix bundle, AN5, the pore waters of which behave rather differently from those of the other systems, simulations at higher external field strengths were also run. For the two pore systems (i.e., AN5 and BN8S8), longer simulations were run at lower values of E_{EXT}. For R6L60, relatively short simulations sufficed to reveal the polarization of the water.

Simulations at low E_{EXT}

We first consider the response of the various channel models to a fairly small external electric field, typically 20 mV/Å. Although we refer to 20 mV/Å as a "low" electric field strength, it corresponds to a voltage drop of ~600 mV across the thickness (~30 Å) of a lipid bilayer. Cell membranes generally have a voltage drop of ~100 mV from the outside to the inside of the cell (Hille, 1992). Furthermore, imposing a voltage difference of significantly more than ~200 mV across a lipid bilayer generally leads to dielectric breakdown of the membrane (Freeman et al., 1994; Weaver and Chizmadzhev, 1996). Thus what is a "low" E_{EXT}, in the context of this paper, is somewhat higher than would be experienced by an ion channel in "real life." However, as will become apparent, it is small in comparison with the protein field that is present in the helix bundle model, which has a dramatic effect on the water's behavior. Note that a positive polarity for E means that V increases as z increases (see Fig. 1).

Three 500-ps MD simulations were carried out for BN8S8: one without a transpore external electric field, and two with the same external E-field strength (20 mV/Å) but with opposite polarities (Table 2). The results of these simulations, in terms of orientational polarization of the pore waters, are illustrated in Fig. 3 *A*. This shows the behavior as a function of time of the z-axis projection of the average dipole of those water molecules that lie within the pore (as defined by the z coordinate of their O atoms lying within $|z| < 15$ Å). In the absence of an external electric field, the value of $\langle \mu_Z \rangle$ fluctuates around zero, as would be expected for the randomly oriented waters seen within a β-barrel pore (Breed et al., 1996). When a positive E_{EXT} is applied, the waters align with their dipoles antiparallel to the pore, so that $\langle \mu_Z \rangle$ adopts a value of about -0.5 D. When E_{EXT} is negative, the waters align in the opposite orienta-

TABLE 2 Polarization of water within pores

System	E_{EXT} (mV/Å)	t (ps)	$\langle\mu_Z\rangle$ in pore (D)	$\langle P_Z\rangle$ in pore (D/Å^3)
BN8S8	0	100 to 500	−0.04 (±0.15)	−0.001 (±0.05)
	+20	100 to 500	−0.57 (±0.12)	−0.019 (±0.004)
	−20	100 to 500	+0.69 (±0.15)	+0.023 (±0.005)
AN5	0	100 to 500	+1.53 (±0.10)	+0.051 (±0.003)
	+20	100 to 500	+1.35 (±0.13)	+0.045 (±0.004)
	+50	100 to 300	+1.32 (±0.13)	+0.044 (±0.004)
	+60	150 to 300	+0.25 (±0.18)	+0.008 (±0.006)
	+75	150 to 300	−0.53 (±0.17)	−0.018 (±0.006)
	+100	150 to 300	−1.44 (±0.15)	−0.048 (±0.005)
	+200	25 to 100	−1.94 (±0.09)	−0.065 (±0.003)
R6L60*	0	15 to 55	+0.08 (±0.14)	+0.003 (±0.005)
	+13.3	20 to 100	−0.47 (±0.14)	−0.016 (±0.005)
	+20	20 to 100	−0.68 (±0.15)	−0.023 (±0.005)
	−20	20 to 100	+0.63 (±0.14)	+0.021 (±0.005)

*Waters for which $|z| < 10$ Å was treated as a "pore" water for the purpose of this analysis.

tion. The alignment of the waters in the applied field (which was not present during the initial energy minimization) takes between 50 and 100 ps. It appears that $\langle\mu_Z\rangle$ is an exactly asymmetrical function of E_{EXT} for BN8S8, suggesting that $E_p = 0$ for this system. As the waters within the BN8S8 pore are relatively free to realign in an external E-field, at a qualitative level this implies a relatively high value of ϵ_{LOCAL} for this system. The behavior of water in the R6L60 cavity is similar to that of the β-barrel model (Table 2).

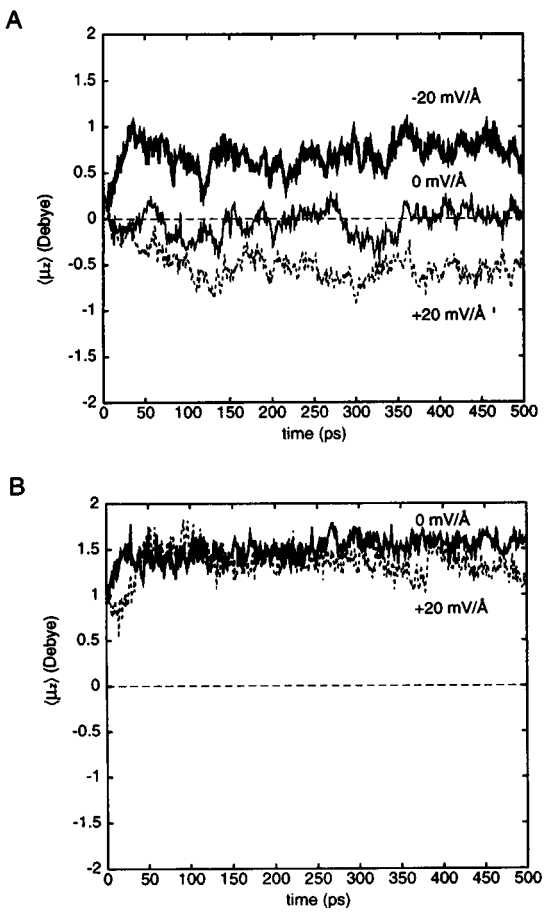

FIGURE 3 Simulations at low E_{EXT}. The mean value of the projection of the dipole moment along the z axis for water molecules within the pore region (i.e., zone 2) as a function of time and of applied E-field strength is shown for (*A*) model BN8S8 and (*B*) model AN5.

The alignment of the pore water dipoles for the α-helix bundle AN5, in the absence and in the presence of a low E_{EXT}, is shown in Fig. 3 *B*. First consider the situation in the absence of an external electric field. As described in previous papers (Breed et al., 1996; Mitton and Sansom, 1996), the water dipoles rapidly (<50 ps) align antiparallel to the α-helix dipoles, i.e., such that $\langle\mu_Z\rangle$ is about +1.5 D. In contrast to the situation for BN8S8, application of an E_{EXT} of 20 mV/Å results in only a small degree of realignment of the pore water dipoles for AN5. Thus, again at a qualitative level, this suggests that water within the AN5 pore is behaving as if it has a relatively low dielectric constant, probably because it is being saturated by the high field from the helix dipoles. However, to analyze the results qualitatively in the framework provided by Eqs. 1 and 4, it is necessary to know E_p, and it is not clear from these simulations what E_p is for AN5, although it is evident that $E_p \neq 0$.

The extent of orientational polarization of the pore waters by low E_{EXT} is compared for the three different systems in Table 2. From this it can be seen that 1) water within the BN8S8 pore is polarized by external electric fields of magnitude 20 mV/Å to about the same extent as water within the central 20 Å (thus avoiding any "end effects") of the 60-Å-long cylinder of water (R6L60); and 2) water within the AN5 pore changes its degree of alignment to a minimal extent (from $\langle P_Z\rangle$ = +0.051 to +0.045 D/Å^3) in response to the same low E_{EXT}. Analysis of these changes in polarization in terms of dielectric constants is described below.

Simulations at high E_{EXT}: further investigation of the AN5 model

To further investigate the dielectric properties of the water within the AN5 pore, MD simulations were run at higher external electric fields (Table 1); the highest field corre-

sponds to a voltage drop of 6 V along a 30-Å channel. The duration of these simulations could be shortened as E_{EXT} was increased because the time required for the system to relax to its new equilibrium decreased as the field strength increased. The motivation for these simulations is to confirm that water in the AN5 pore is indeed described by Eq. 1, by applying fields of sufficient strength so as to be able to measure the polarization of the water over a range comparable to that shown in Fig. 1.

First examine the two extremes. In Fig. 4 *A* the value of μ_Z for each water molecule is plotted as a function of the z coordinate of the water O atom, for a snapshot of the zero-E_{EXT} simulation taken at t = 100 ps. As discussed before (Breed et al., 1996), the water dipoles within the pore are aligned antiparallel relative to the α-helix dipoles. There is also some small degree of alignment (in the opposite direction, as expected) in the caps at either mouth of the pore, although this is less statistically significant. If one examines the equivalent graph for the AN5 simulation after 100 ps of the highest E_{EXT} (+200 mV/Å), it can be seen that all of the waters, both within and at the mouths of the pore, are aligned by the external E field. There is no difference between pore and caps, and thus in the presence of this very strong external E field, the helix dipoles have no perceptible influence on the alignment of the water dipoles.

The equivalent graphs of μ_Z versus z for intermediate values of E_{EXT} are shown in Fig. 4 *C*. It can be seen that E_{EXT} = +50 mV/Å has little effect on the alignment of waters within the pore, whereas at +75 mV/Å the pore waters have started to realign in the external field. Of course, it should be remembered that these graphs provide only an instantaneous picture of the system. However, they do reveal that for a given value of E_{EXT} there is some variation along the length of the pore in the extent of realignment of the water dipoles.

The evolution with respect to time of $\langle \mu_Z \rangle$ for waters in the pore region of AN5 at different E_{EXT} is shown in Fig. 5 *A*. From this, two features are evident: 1) the change in equilibrium polarization of the pore waters increases as E_{EXT} increases; and 2) the rate of relaxation of $\langle \mu_Z \rangle$ to its new equilibrium value is faster for higher external E field strengths. Thus, for the +75 and +100 mV/Å fields, realignment of the water dipoles is not complete until ~150 ps, whereas for +200 mV/Å the change is completed within the heating and equilibration stages (i.e., within 15 ps). The corresponding values of $\langle P_Z \rangle$ once the dipole realignment is complete are listed in Table 2. It is evident that the dielectric behavior of the pore water of AN5 as E_{EXT} is increased is nonlinear in nature. However, this behavior is much more easily understood if the polarization is considered as a function of E_{TOT} rather than E_{EXT}, as is done in the next section.

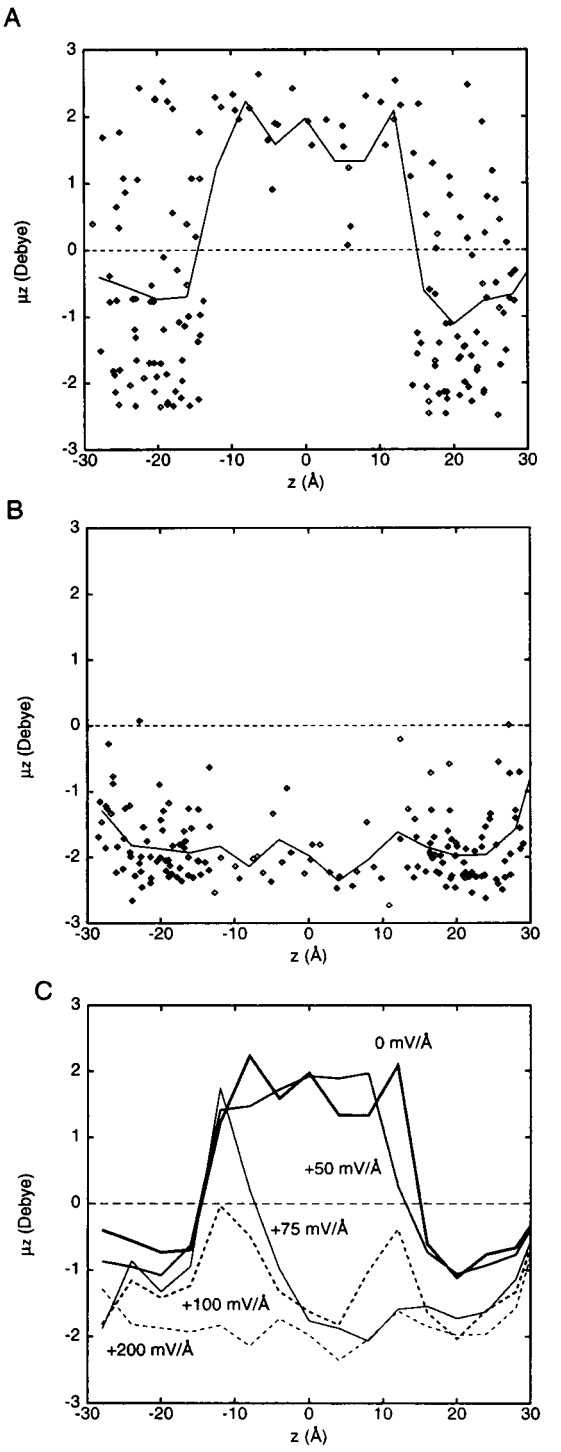

FIGURE 4 Effect of high E_{EXT} on water dipole orientation profiles for model AN5. (*A* and *B*) Water dipole orientation profiles for the simulations with E_{EXT} = 0 and E_{EXT} = +200 mV/Å, respectively. In both cases the profiles correspond to the system at the end of 100 ps of MD. Each point corresponds to μ_Z for a single water molecule; the lines correspond to the smoothed profiles. (*C*) Smoothed profiles for simulations with E_{EXT} = 0, +50, +75, +100, and +200 mV/Å.

Estimation of ϵ_{LOCAL}

A change in polarization as a function of external E field may be used to estimate the local dielectric of water within

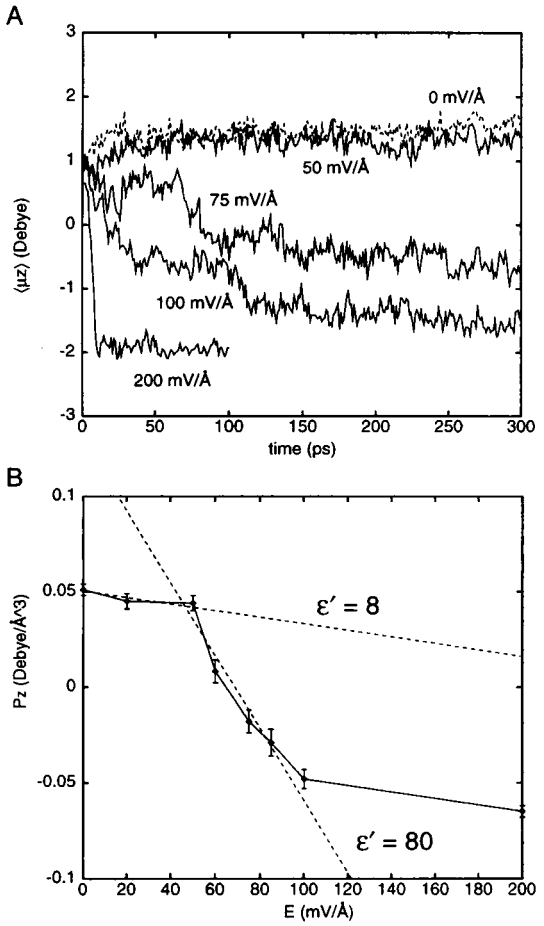

FIGURE 5 Pore water polarization as a function of E_{EXT} for model AN5. (*A*) The mean value of the projection of the dipole moment along the z axis for water molecules within the pore region (i.e., zone 2) as a function of time for different applied E-field strengths. (*B*) The mean polarization along z within the pore as a function of E_{EXT}. Each point represents the average (± SD) of the polarization along z of all water molecules within the pore, averaged as described in Table 2. The two straight lines, with slopes corresponding to $\epsilon' = 8$ and $\epsilon' = 80$, were fitted to the data points for the low-E_{EXT} (0–50 mV/Å) and high-E_{EXT} (50–100 mV/Å) regions.

a pore, ϵ_{LOCAL}. Concentrating first on the two systems that showed appreciable reorientation of water molecules in response to a small E_{EXT}, i.e., BN8S8 and R6L60 (Table 2), this can be used to estimate ϵ_{LOCAL}. For the cylindrical cavity, R6L60, to avoid possible end effects, "pore" water was defined as that within the central 20 Å of the 60-Å-long cylinder, i.e., $|z| < 10$ Å. In both cases, the dependence of orientational polarization on the external electric field strength suggested that $\epsilon_{LOCAL} \approx 40$ (Table 3). This is only half of the value for "bulk" water; the significance of this is discussed below.

The behavior of water within the AN5 pore is more complex. In particular, the polarization is a nonlinear function of E_{EXT}. However, mapping out the graph of $\langle P_Z \rangle$ versus E_{EXT} for values of E_{EXT} much higher than would be found in nature enables us to estimate the value of E_p from Fig. 5 *B* by using the fact that $\langle \mu_Z \rangle = 0$, where $E = 0$, i.e.,

TABLE 3 Dielectrics of water within pores

System	ϵ'_{LOCAL}
BN8S8, pore	41
AN5, pore, low E_{EXT}	8
AN5, pore, high E_{EXT}	80
R6L60, "pore"	44

where $E_p = -E_{EXT}$. Then it is clear that if Fig. 5 *B* were replotted as a function of $E = E_{EXT} + E_p$, the apparent discrepancy with Fig. 1 would disappear, showing that Eq. 1 decribes the behavior of water in all of the systems studied, provided that all contributions to E are included. The best estimate for E_p is $E_p \approx -65$ mV/Å, although it is clear from Fig. 4 *C* that the field is not uniform. Nevertheless, E_P is approximately the same throughout the pore, and thus the estimation of a single ϵ_{LOCAL} within the pore is appropriate, justifying a posteriori our assumption that an analysis of this kind would be appropriate. Having made this identification, we can use Eqs. 5 and 7 to define effective dielectric constants. Fig. 5 *B* suggests that there are two interesting modes of behavior of pore water for AN5. First let us consider the case where $E_{EXT} \approx 0$, and so expand about $E_0 = -E_p$. In this case, the water's polarization is nearly saturated because of the strong protein electric field. Using Eqs. 5 and 7, it is found that $\epsilon'_{LOCAL} \approx 8$, whereas $\epsilon_{LOCAL} \approx 30$. ϵ'_{LOCAL} does not in fact alter very much for any "low" E_{EXT}, up to approximately +50 mV/Å. The second case of interest is where E_{EXT} is much higher (+50 mV/Å to +100 mV/Å) so $E \approx 0$, and we expand about $E_0 = 0$. Here the polarization changes more rapidly with increasing E, corresponding to $\epsilon_{LOCAL} \approx \epsilon'_{LOCAL} \approx 80$, and Eqs. 5 and 7 are nearly equivalent. As E_{EXT} is increased further, dielectric saturation is eventually reached again (at $E_{EXT} = +200$ mV/Å). Note that the upper limit for "low" E_{EXT} behavior of the AN5 pore water (+50 mV/Å) corresponds to a voltage difference of 1500 mV across a 30-Å-thick membrane, i.e., more than an order of magnitude greater than the voltage difference across a cell membrane due to ionic concentration gradients. Thus, in most situations, one might expect the water within a transbilayer pore formed by a parallel bundle of α-helices to behave as a relatively low dielectric medium, with significant consequences for the strength of electrostatic interactions within such a pore. It is perhaps also worth noting that E near an ion is of this order of magnitude (Jayaram et al., 1989; Partenskii and Jordan, 1992a). The effect that this might have on the water will be discussed later.

Effects of ϵ_{LOCAL}

Having shown that for model AN5, the value of ϵ_{LOCAL} is dependent on its definition and on E_{EXT}, it is important to consider the value of ϵ_{LOCAL} to be used in calculations, and then to estimate the effect of changing the value of ϵ_{LOCAL}

on the results of such calculations. Such considerations require a small theoretical digression. The Poisson equation

$$\nabla \cdot \epsilon \nabla \phi = -\frac{\rho_F}{\epsilon_0} \tag{8}$$

where ρ_F refers to fixed charges only, is derived from the Maxwell equation

$$\nabla \cdot E = -\frac{\rho_{TOTAL}}{\epsilon_0} \tag{9}$$

by assuming that all polarization charges are related linearly to the total E field by a (possibly spatially varying) dielectric constant. If it is to be used in the case where E (i.e., E_{TOT}) is large, then an appropriate effective dielectric should be used that captures either the local linear behavior or the average behavior of $P(E)$ as E increases from 0. For example, to estimate the electrostatic energy of an ion as it passes down the pore, Eq. 8 should be used with $\epsilon = \epsilon_{LOCAL}$ as defined by Eq. 7, because the quantity that is of interest in this case is the total quantity of polarization charge that accumulates in the channel as E increases from 0 to E_0 (see *line 2* in Fig. 2). Conversely, if the energy of interaction of two ions in the channel is of interest, as may be the case in Poisson-Nernst-Planck calculations of conductance, then it is the change in polarization produced by extra charge that is required and the differential definition of $\epsilon'_{LOCAL}(E)$ from Eq. 5 is appropriate (see *line 1* in Fig. 2). This can be seen by direct substitution; suppose we have calculated a potential ϕ_0, corresponding to a field E_0, appropriate to a channel containing some distribution of fixed charges, and we then add some extra fixed charge $\Delta\rho$. The extra polarization charge due to this is given by Eq. 5, and on substituting into the Maxwell equation Eq. 9, a Poisson equation for the change in electrical potential $\Delta\phi$ is obtained:

$$\nabla \cdot \epsilon'_{LOCAL} \nabla(\Delta\phi) = -\frac{\Delta\rho}{\epsilon_0} \tag{10}$$

Thus, $\epsilon'_{LOCAL}(E)$ for ion-ion interactions is ~8, but ϵ_{LOCAL} for the energy of a permeant ion is ~30 (Eq. 7). It should be noted that all of this analysis has been carried out for the Poisson equation, rather than the PB equation, which also includes the effects of ionic screening. It would be possible to perform the same kind of analysis, in which case the inverse screening length, κ, would also be a function of E, via the effect of the latter on ϵ_{LOCAL}. However, we prefer to treat the effects of ion-ion interactions by way of Eq. 10.

One may try to understand the consequences of a low value of ϵ_{LOCAL} by a simple continuum electrostatics calculation on pore model AN5. Note that we are not proposing that such calculations are sufficient to accommodate all aspects of channel electrostatics, but simply using such a calculation as an example of the importance of ϵ_{LOCAL}. As described above, the pore model was embedded in a low-dielectric ($\epsilon = 2$) slab representing a membrane, and the solvent regions on either side were assigned a dielectric of 78. The PB equation was solved numerically to yield an estimate of the electrostatic potential along the length of the pore for different values of ϵ_{LOCAL}. For convenience, the pore electrostatic energy profile can be expressed as the potential energy of a $+1e$ probe charge placed at successive points along the length of the channel, although it should be stressed that this is simply a way of converting from mV to kcal/mol and does not take into account the effect of a permeant cation on the local electrostatic field.

Two alternative values have been explored for the dielectric of water within the pore. The default assumption is that pore water behaves much the same as bulk water, i.e., that $\epsilon_{LOCAL} = 78$. The second approach is to employ the estimate of $\epsilon_{LOCAL} \approx 30$, i.e., the value for the energy of a single permeant ion.

The consequences of these two different values of the local dielectric within the pore may be displayed (Fig. 6) in terms of an electrostatic potential energy profile calculated along the length of the AN5 pore by numerical solution of the Poisson-Boltzmann equation (strictly, solution of the Poisson equation, as zero ionic strength has been assumed in this calculation, for the sake of simplicity). In both cases there is a potential energy barrier at the N-terminal mouth and a potential energy well at the C-terminal mouth, as a result of the parallel α-helix dipoles. The height/depth of the barrier/well is strongly dependent on the value of ϵ_{LOCAL} assumed. Thus, if one assumes $\epsilon_{LOCAL} = 78$, the barrier/well magnitude is ~$7RT$. This rises to ~$13RT$ if one assumes that $\epsilon_{LOCAL} = 30$. Of course, this calculation is rather simplistic, and a more complete theoretical treatment will need to be developed to address the energetics of permeation of an ion or ions. However, the results reveal that the value of ϵ_{LOCAL} may have a significant effect.

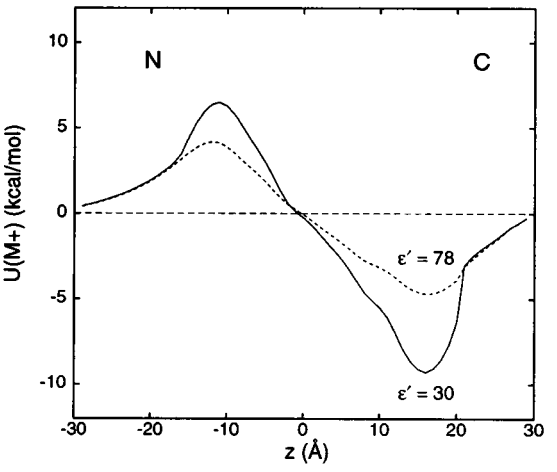

FIGURE 6 Effect of ϵ_{LOCAL} on the electrostatic potential energy profile along the z axis of the pore, the latter being calculated via numerical solution of the Poisson-Boltzmann equation (see text). The profiles correspond to $\epsilon_{LOCAL} = 78$ (– – –) and $\epsilon_{LOCAL} = 30$ (——).

DISCUSSION

Methodology

There are two main methods of estimation of dielectric constants by MD simulations. The first involves running extended MD simulations and analyzing the equilibrium fluctuation in the total dipole moment of a system. The second method (as in the current study) involves using MD simulations to measure the polarization response to an applied electrostatic field. The two approaches are related by the fluctuation-dissipation theorem. A medium with a high dielectric susceptibility, i.e., one that undergoes substantial reorientation of its dipoles in response to an applied E field, will also exhibit large equilibrium fluctuations in the orientation of those dipoles. In fact, the fluctuation-dissipation theorem also describes the response to time-varying fields, going rather beyond the studies made here, where the applied field is static.

Both methods have been employed extensively to estimate the dielectric constant of water from MD simulations. The dipole fluctuation approach has been explored in some detail by Neumann (1986) and more recently by Simonson (1996), and has been shown to be capable of yielding accurate estimates of ϵ for water. The alternative method, based on the response to an external E field, was pioneered by Watts (1981a,b). A comparison of these methods applied to water (Alper and Levy, 1989) confirmed that both yield accurate estimates of ϵ, provided that long-range forces are properly treated. For example, in the latter study it was shown that use of a cutoff of ~8 Å for long-range forces reduced the dielectric constant estimate for bulk water to ~25.

Such approaches have been extended to MD simulation studies of proteins, both in vacuo and in solvent droplets (e.g., King et al., 1991). In particular, Simonson and colleagues (Simonson and Perahia, 1995a,b) have employed analysis of equilibrium fluctuations in the total dipole to demonstrate that the dielectric constant of a protein varies spatially, rising from $\epsilon = 2$–3 in the interior of a protein to $\epsilon = 10$–20 at its surface. The dielectric response of bovine pancreatic trypsin inhibitor, in vacuo, to an external electrostatic field has been explored by Xu et al. (1996).

To the best of our knowledge this is the first time that simulation methods have been used in this way to analyze the dielectric constant of water within a model ion channel. The studies cited above provide confidence in such an approach. However, it is important to consider the limitations of the current simulations. The first limitation is the use of a simple three-point charge model of water, i.e., TIP3P. However, although more complex water models are available, encouragement may be derived from the results of Simonson (1996), who showed that MD simulations of a droplet of TIP3P water yielded a dielectric of ~80 for the bulk solvent. The second limitation is the relative neglect of long-range interactions. A number of simulation studies of water (see above) suggest that such neglect may lead to underestimation of ϵ, perhaps explaining why we obtain $\epsilon = 40$ for the β-barrel pore model.

The use of the method of simulating the response to an external electrostatic field and the neglect of long-range interactions in the current study are interlinked. In simulations of globular proteins, analysis of the fluctuations in the total dipole moment is carried out using the Fröhlich-Kirkwood theory, with the system treated as a sphere surrounded by a medium of homogeneous dielectric. Our system is nonspherical, and the surrounding medium (bilayer plus water on either side of the bilayer) is markedly inhomogeneous in its dielectric properties. The inherent asymmetry of the system suggests that measuring the response of the water dipoles to a transpore external field is a natural approach to the dielectric properties of the water within the pore. The relative neglect of long-range interactions (a cutoff of 13 Å was applied in our simulations) is anticipated to reduce the estimated dielectric constants somewhat. However, the effect may not be too extreme. In his simulation studies of spherical water droplets in vacuo, Simonson (1996) noted that polar fluctuations in the inner half of the droplet were bulklike, despite the surrounding vacuum, because of efficient screening by the outer half of the droplet. In our system we have focused on the inner "pore" waters of the system, which are electrostatically screened from the surrounding vacuum by either protein atoms of the channel lining or by the caps of water at either channel mouth. We are thus reasonably confident that our method will yield a useful first approximation to the dielectric properties of pore water. In any case, there is no reliable technique for correcting for the neglect of long-range interactions, because reaction-field techniques assume a constant dielectric outside the cutoff range. One possible check on the effect of the cutoffs is to compare the estimate of $E_p \approx -65$ mV/Å from the MD calculation with the gradient of the potential energy profile from the Poisson-Boltzmann calculation in Fig. 6. This gradient (calculated with an effective ϵ of 30) corresponds to a field strength of about -25 mV/Å, which is appreciably different from the MD estimate. Although the PB treatment is, of course, itself approximate, and is not in any case independent of the MD calculation that was used to estimate ϵ, this discrepancy is large enough to point to the necessity for further simulations with a more careful treatment of long-range electrostatics. However, as the crux of the analysis is based on the comparison of AN5 with BN8S8 and R6L60, even if absolute values of ϵ are in error, the values for one system relative to another are likely to be correct.

Analysis

Here we comment briefly on the possible deficiencies of the analytical framework, based on Eq. 1, in which the results have been analyzed. Equation 1 accounts for the nonlinearity of the response P to the field E, but it does not include possible nonlocalities, that is to say, it is assumed that the

polarization at a point, $P(r)$, depends only on $E(r)$ at the same point, i.e., $P(r) = f(E(r))$. In fact it is possible (and, for this system, likely) that fields at neighboring points could contribute: i.e., in general, $P(r) = f(\int \epsilon(r, r')E(r')dr')$ (Partenskii and Jordan, 1992a). An equation of this form can be viewed as describing the correlations between water molecules due to hydrogen bonding. We have not attempted to estimate the quantitative effect that such nonlocalities would have, mainly for practical reasons: estimating the kernel of an integral equation (i.e., estimating $\epsilon(r, r')$ above) is an extremely difficult problem because the inversion tends to be very unstable. However, we point out that, by "smearing" out the effective local electric field, the qualitative effect of nonlocalities is probably to improve the accuracy of the empirical assignment of a spatially invariant dielectric constant to the whole of the pore. It should also be noted that correlations between water molecules that cause them to behave effectively as "clusters" do not affect the form of Eq. 1, but only cause it to be scaled; deviations in functional form only arise if the size of the clusters varies with E. (Indeed, the observed ϵ can be used to estimate the extent of clustering: for water with $E_{TOT} = 0$, $\epsilon = 78$ implies, plausibly, that the water molecules move effectively in groups of four).

Implications

The main result from our simulations is that the dielectric behavior of water within transbilayer pores formed by parallel bundles of α-helices is predicted to differ significantly from that of bulk water. Our analysis suggests that for calculations of ion-ion interactions within a pore, a value of $\sim$8 should be employed, whereas for calculations of the change in electrostatic energy for a single permeant ion, a value of $\sim$30 for the pore dielectric may be more appropriate.

How general is this reduction of ϵ_{LOCAL} likely to be? The simulations of AN5 at high E_{EXT} reveal the source of the low dielectric constant of the pore water in this system, namely the alignment of the water molecules antiparallel to the helix dipoles. Simulations on rather less idealized models of pores formed by bundles of parallel α-helices, e.g., alamethicin, δ-toxin (Breed et al., 1996), de novo designed amphipathic peptides (Mitton and Sansom, 1996), and the pore domain of the nicotinic acetylcholine receptor (Smith and Sansom, 1997), suggest that in all of these systems, in which the pore is lined with a variety of charged and polar side chains, the dipoles of the pore waters are aligned by the local electric field created by the helix dipoles and the side chains. Thus one might anticipate a significant reduction of the dielectric constant of water within all channels in which the pore is lined by a parallel bundle of α-helices (Oiki et al., 1990). The extent of this reduction, which is a function of E_p, might be expected to depend largely on "geometrical" parameters such as the diameter and supercoiling of the bundle, and to be fairly robust to changes in sequence.

This phenomenon may not be limited to channels formed by α-helix bundles. Alignment of pore water dipoles is expected to occur within any narrow channel with a significant electric field E_p created by the backbone and/or side-chain atoms of the pore-lining residues. For example, simulations (Ranatunga, Kerr, and Sansom, unpublished results) on models of K^+ channel pores formed by β-barrels suggest that, even in the absence of a helix dipole, the local E field created by, e.g., charged side chains at a mouth of a pore may significantly align the dipoles of water molecules within the pore. Furthermore, x-ray (Weiss et al., 1991; Cowan et al., 1992) and theoretical (Karshikoff et al., 1994) studies of bacterial porins have stressed the presence of a strong transverse electric field in the narrowest region of the pore. Interestingly, one of the few experimental estimates of the dielectric constant for pore water suggests that for water within the pore of the porin PhoE, the dielectric is $\sim$20 (Gutman et al., 1992). Application of a similar experimental technique to water within the heme-binding pocket of apomyoglobin yields a dielectric of $\sim$9 (Shimoni et al., 1993), and application to water within a hexagonal phase phospholipid tube (radius $\sim$10 Å) yields a value of $\sim$30 (Fried et al., 1995). Although the relationship of these indirect experimental estimates to ϵ'_{LOCAL} as defined above is uncertain, these experiments do indicate that the dielectric properties of water within a pore or cavity differ from those of bulk water.

The importance of a low value of the dielectric within a pore on the energetics of permeation of the pore by ions is illustrated by the PB calculations on AN5. Although these calculations represent a somewhat crude approach to ion permeation energetics, they do suggest that analysis of the importance of α-helix dipoles to the potential energy profile of a channel (Chen et al., 1997) may depend crucially on the assumed dielectric constant of water within the pore. In the context of water within a model of gramicidin channels, Jordan and colleagues (Partenskii and Jordan, 1992a) have also emphasized the importance of correct treatment of the dielectric properties of the pore water.

As well as considering the effect of the dielectric constant on the electric field experienced by an ion due to fixed charges on the channel protein, one should also consider the strength of the electric field produced by an ion itself in the channel environment. A useful measure of this is the distance from an ion at which E_{ion} and E_p are equal: although no explicit ions were included in this investigation, the results suggest that $E_{ion} = E_p$ in the AN5 model $\sim$5 Å from the ion, using Coulomb's law for the ion with $\epsilon' = 8$, and $E_p = 65$ mV/Å. This is in agreement with the results of simulations (including explicit ions) of models of the M2 helix bundle of the nicotinic acetylcholine receptor, in which it was found that the water dipoles were more strongly oriented by the ion than by the dipole field only in the first coordination shell, less than 4 Å from the ion (Smith and Sansom, 1997). However, even more than the AN5 and BN8S8 models, the acetylcholine receptor model has a wide pore; the effect of the ion's field probably depends on the channel geometry, and the situation is likely to be very different in very narrow pores. In particular,

many studies of gramicidin have pointed to a very strong effective field from the ion in this system, which orients the waters throughout the pore (Partenskii and Jordan, 1992a). The effective strength of ion-ion interactions is probably comparable to this ion-water effect.

These simulations provide an insight into the complex dielectric behavior of water, even within a simplified model protein environment. There are two directions that such studies now follow. The first is to improve the simulation methodology to improve estimates of ϵ_{LOCAL} for a range of different ion channels. In particular, attention must be paid to the sensitivity of the results to the water model, and to treatment of long-range interactions. The latter may require simulations on more complex systems, i.e., channel plus water plus bilayer (Lee et al., 1995; Woolf and Roux, 1996). The second direction is to extend such investigations to nonmembrane proteins that contain "immobilized" water molecules, such as the five-helix bundle protein COMP (Malashkevich et al., 1996). Improved characterization of the dielectric properties of water within pockets and at the surface of protein may result in improved PB calculations of protein electrostatics (Warwicker, 1994) and improved prediction of conductance properties (Chen et al., 1997; Smart et al., 1997).

This work was supported by a grant from the Wellcome Trust. PB is an MRC research student. Our thanks also to the Oxford Centre for Molecular Sciences for access to computational facilities, and to our colleagues for helpful comments on this work.

REFERENCES

Adams, P. D., I. T. Arkin, D. M. Engelman, and A. T. Brünger. 1995. Computational searching and mutagenesis suggest a structure for the pentameric transmembrane domain of phospholamban. *Nature Struct. Biol.* 2:154–162.

Alper, H. E., and R. M. Levy. 1989. Computer simulations of the dielectric properties of water: studies of the simple point charge and transferrable intermolecular potential models. *J. Chem. Phys.* 91:1242–1251.

Åqvist, J., and A. Warshel. 1989. Energetics of ion permeation through membrane channels: solvation of Na^+ by gramicidin A. *Biophys. J.* 56:171–182.

Arkin, I. T., M. Rothman, C. F. C. Ludlam, S. Aimoto, D. M. Engelman, K. J. Rothschild, and S. O. Smith. 1995. Structural model of the phospholamban ion channel complex in phospholipid membranes. *J. Mol. Biol.* 248:824–834.

Biggin, P. C., and M. S. P. Sansom. 1996. Simulation of voltage-dependent interactions of α-helical peptides with lipid bilayers. *Biophys. Chem.* 60:99–110.

Breed, J., P. C. Biggin, I. D. Kerr, O. S. Smart, and M. S. P. Sansom. 1997. Alamethicin channels—molecular modelling via restrained molecular dynamics simulations. *Biochim. Biophys. Acta.* 1325:235–249.

Breed, J., R. Sankararamakrishnan, I. D. Kerr, and M. S. P. Sansom. 1996. Molecular dynamics simulations of water within models of transbilayer pores. *Biophys. J.* 70:1643–1661.

Brooks, B. R., R. E. Bruccoleri, B. D. Olafson, D. J. States, S. Swaminathan, and M. Karplus. 1983. CHARMM: a program for macromolecular energy, minimisation, and dynamics calculations. *J. Comp. Chem.* 4:187–217.

Chen, D., J. Lear, and B. Eisenberg. 1997. Permeation through an open channel: Poisson-Nernst-Planck theory of a synthetic ionic channel. *Biophys. J.* 72:97–116.

Chiu, S. W., E. Jakobsson, S. Subramanian, and J. A. McCammon. 1991. Time-correlation analysis of simulated water motion in flexible and rigid gramicidin channels. *Biophys. J.* 60:273–285.

Cowan, S. W., T. Schirmer, G. Rummel, M. Steiert, R. Ghosh, R. A. Pauptit, J. N. Jansonius, and J. P. Rosenbusch. 1992. Crystal structures explain functional properties of two *E. coli* porins. *Nature.* 358:727–733.

Davis, M. E., J. D. Madura, B. A. Luty, and J. A. McCammon. 1991. Electrostatics and diffusion of molecules in solution: simulations with the University of Houston Brownian dynamics program. *Comput. Phys. Comm.* 62:187–197.

Engel, A., T. Walz, and P. Agre. 1994. The aquaporin family of membrane water channels. *Curr. Opin. Struct. Biol.* 4:545–553.

Engels, M., D. Bashford, and M. R. Ghadiri. 1995. Structure and dynamics of self-assembling peptide nanotubes and the channel-mediated water organization and self-diffusion. A molecular dynamics study. *J. Am. Chem. Soc.* 117:9151–9158.

Freeman, S. A., M. A. Wang, and J. C. Weaver. 1994. Theory of electroporation of planar bilayer-mebranes—prediction of the aqueous area, change in capacitance, and pore-pore separation. *Biophys. J.* 67:42–56.

Fried, O., E. Nachliel, and M. Gutman. 1995. Time resolved measurements of proton diffusion in HexII water-phospholipids mixture. *Solid State Ionics.* 77:84–88.

Green, M. E., and J. Lewis. 1991. Monte Carlo simulation of the water in a channel with charges. *Biophys. J.* 59:419–426.

Gutman, M., Y. Tsfadia, A. Masad, and E. Nachiel. 1992. Quantitation of physical-chemical properties of the aqueous phase inside the phoE ionic channel. *Biochim. Biophys. Acta.* 1109:141–148.

Hille, B. 1992. Ionic Channels of Excitable Membranes, 2nd. ed. Sinauer Associates. Sunderland, MA.

Jayaram, B., R. Fine, K. Sharp, and B. Honig. 1989. Free energy calculations of ion hydration: an analysis of the Born model in terms of microscopic simulations. *J. Phys. Chem.* 93:4320–4327.

Jorgensen, W. L., J. Chandresekhar, J. D. Madura, R. W. Impey, and M. L. Klein. 1983. Comparison of simple potential functions for simulating liquid water. *J. Chem. Phys.* 79:926–935.

Karshikoff, A., V. Spassov, S. W. Cowan, R. Ladenstein, and T. Schirmer. 1994. Electrostatic properties of two porin channels from *Escherichia coli. J. Mol. Biol.* 240:372–384.

Kerr, I. D., D. G. Doak, R. Sankararamakrishnan, J. Breed, and M. S. P. Sansom. 1996. Molecular modelling of staphylococcal δ-toxin ion channels by restrained molecular dynamics. *Protein Eng.* 9:161–171.

Kerr, I. D., J. Dufourcq, J. A. Rice, D. R. Fredkin, and M. S. P. Sansom. 1995. Ion channel formation by synthetic analogues of staphylococcal δ-toxin. *Biochim. Biophys. Acta.* 1236:219–227.

King, G., F. S. Lee, and A. Warshel. 1991. Microscopic simulations of macroscopic dielectric constants of solvated proteins. *J. Chem. Phys.* 95:4366–4377.

Kraulis, P. J. 1991. MOLSCRIPT: a program to produce both detailed and schematic plots of protein structures. *J. Appl. Crystallogr.* 24:946–950.

Kreusch, A., and G. E. Schulz. 1994. Refined structure of the porin from *Rhodobacter blastica. J. Mol. Biol.* 243:891–905.

Lee, K. C., S. Huo, and T. A. Cross. 1995. Lipid-peptide interface: valine conformation and dynamics in the gramicidin channel. *Biochemistry.* 34:857–867.

Lynden-Bell, R., and J. C. Rasaiah. 1996. Mobility and solvation of ions in channels. *J. Chem. Phys.* 105:9266–9280.

Malashkevich, V. N., R. A. Kammerer, V. P. Efimov, T. Schulthess, and J. Engel. 1996. The crystal structure of a five-stranded coiled coil in COMP: a prototype ion channel? *Science.* 274:761–765.

Mellor, I. R., D. H. Thomas, and M. S. P. Sansom. 1988. Properties of ion channels formed by *Staphylococcus aureus* δ-toxin. *Biochim. Biophys. Acta.* 942:280–294.

Mitton, P., and M. S. P. Sansom. 1996. Molecular dynamics simulations of ion channels formed by bundles of amphipathic α-helical peptides. *Eur. Biophys. J.* 25:139–150.

Montal, M. 1995. Design of molecular function: channels of communication. *Annu. Rev. Biophys. Biomol. Struct.* 24:31–57.

Neumann, M. 1986. Dielectric relaxation in water. Computer simulations with the TIP4P potential. *J. Chem. Phys.* 85:1567–1580.

Oiki, S., V. Madison, and M. Montal. 1990. Bundles of amphipathic transmembrane α-helices as a structural motif for ion conducting channel proteins: studies on sodium channels and acetylcholine receptors. *Proteins Struct. Funct. Genet.* 8:226–236.

Partenskii, M. B., and P. C. Jordan. 1992a. Nonlinear dielectric behaviour of water in transmembrane ion channels: ion energy barriers and the channel dielectric constant. *J. Phys. Chem.* 96:3906–3910.

Partenskii, M. B., and P. C. Jordan. 1992b. Theoretical perspectives on ion-channel electrostatics: continuum and microscopic approaches. *Q. Rev. Biophys.* 25:477–510.

Roux, B., and M. Karplus. 1994. Molecular dynamics simulations of the gramicidin channel. *Annu. Rev. Biophys. Biomol. Struct.* 23:731–761.

Sancho, M., M. B. Partenskii, V. Dorman, and P. C. Jordan 1995. Extended dipolar chain model for ion channels: electrostriction effects and the translocational energy barrier. *Biophys. J.* 68:427–433.

Sankararamakrishnan, R., C. Adcock, and M. S. P. Sansom. 1996. The pore domain of the nicotinic acetylcholine receptor: molecular modelling and electrostatics. *Biophys. J.* 71:1659–1671.

Sansom, M. S. P. 1991. The biophysics of peptide models of ion channels. *Prog. Biophys. Mol. Biol.* 55:139–236.

Sansom, M. S. P. 1993a. Alamethicin and related peptaibols—model ion channels. *Eur. Biophys. J.* 22:105–124.

Sansom, M. S. P. 1993b. Structure and function of channel-forming peptaibols. *Q. Rev. Biophys.* 26:365–421.

Sansom, M. S. P., and I. D. Kerr. 1993. Influenza virus M2 protein: a molecular modelling study of the ion channel. *Protein Eng.* 6:65–74.

Sansom, M. S. P., I. D. Kerr, J. Breed, and R. Sankararamakrishnan. 1996. Water in channel-like cavities: structure and dynamics. *Biophys. J.* 70:693–702.

Shimoni, E., Y. Tsfadia, E. Nachiel, and M. Gutman. 1993. Gaugement of the inner space of the apomyoglobin's heme binding site by a single free diffusing proton. *Biophys. J.* 64:472–479.

Simonson, T. 1996. Accurate claculation of the dielectric constant of water from simulations of a microscopic droplet in vacuum. *Chem. Phys. Lett.* 250:450–454.

Simonson, T., and D. Perahia. 1995a. Internal and interfacial dielectric properties of cytochrome c from molecular dynamics in aqueous solution. *Proc. Natl. Acad. Sci. USA.* 92:1082–1086.

Simonson, T., and D. Perahia. 1995b. Microscopic dielectric properties of cytochrome c from moleular dynamics simulations in aqueous solution. *J. Am. Chem. Soc.* 117:7987–8000.

Singh, C., R. Sankararamakrishnan, S. Subramanian, and E. Jakobsson. 1996. Solvation, water permeation, and ionic selectivity of the voltage-gated sodium channel. *Biophys. J.* 71:2276–2288.

Smart, O. S., J. Breed, G. R. Smith, and M. S. P. Sansom. 1997. A novel method for structure-based prediction of ion channel conductance properties. *Biophys. J.* 72:1109–1126.

Smith, G. R., and M. S. P. Sansom. 1997. Molecular dynamics study of water and Na^+ ions in models of the pore region of the nicotinic acetylcholine receptor. *Biophys. J.* 73:1364–1381.

Smith, P. E., R. M. Brunne, A. E. Mark, and W. F. van Gunsteren. 1993. Dielectric properties of trypsin inhibitor and lysozyme calculated from molecular dynamics simulations. *J. Phys. Chem.* 97:2009–2014.

Song, L., M. R. Hobaugh, C. Shustak, S. Cheley, H. Bayley, and J. E. Gouaux. 1996. Structure of staphylococcal α-hemolysin, a heptameric transmembrane pore. *Science.* 274:1859–1866.

Syganow, A., and E. von Kitzing. 1995. Integral weak diffusion and diffusion approximations applied to ion transport through biological ion channels. *J. Phys. Chem.* 99:12030–12040.

Unwin, N. 1989. The structure of ion channels in membranes of excitable cells. *Neuron.* 3:665–676.

Unwin, N. 1993. Nicotinic acetylcholine receptor at 9 Å resolution. *J. Mol. Biol.* 229:1101–1124.

Unwin, N. 1995. Acetylcholine receptor channel imaged in the open state. *Nature.* 373:37–43.

Walz, T., D. Typke, B. L. Smith, P. Agre, and A. Engel. 1995. Projection map of aquaporin-1 determined by electron crystallography. *Nature Struct. Biol.* 2:730–732.

Warshel, A., and J. Åqvist. 1991. Electrostatic energy and macromolecular function. *Annu. Rev. Biophys. Biophys. Chem.* 20:267–298.

Warwicker, J. 1994. Improved continuum electrostatic modelling in proteins, with comparison to experiment. *J. Mol. Biol.* 236:887–903.

Watts, R. O. 1981a. Electric polarization of water: Monte Carlo studies. *Chem. Phys.* 57:185–195.

Watts, R. O. 1981b. Molecular dynamics study of electric polarization. *Chem. Phys. Lett.* 80:211–214.

Weaver, J. C., and Y. A. Chizmadzhev. 1996. Theory of electroporation: a review. *Bioelectrochem. Bioenerg.* 41:135–160.

Weiss, M. S., U. Abele Weckesser, J., W. Welte, E. Schiltz, and G. E. Schulz. 1991. Molecular architecture and electrostatic properties of a bacterial porin. *Science.* 254:1627–1630.

Woolf, T. B., and B. Roux. 1996. Structure, energetics, and dynamics of lipid-protein interactions—a molecular-dynamics study of the gramicidin-A channel in a DMPC bilayer. *Proteins Struct. Funct. Genet.* 24: 92–114.

Xu, D., J. C. Phillips, and K. Schulten. 1996. Protein response to external electric fields: relaxation, hysteresis, and echo. *J. Phys. Chem.* 100: 12108–12121.